HiLL PUBLISHING

Engineering Advances, 2023, 3(5), 407-417
https://www.hillpublisher.com/journals/ea/
ISSN Online: 2768-7961

Considering the Cooperative Guidance Law of Multiple Vehicles in Detection Configuration

Shuo Yuan, Yang Guo*, Shaobo Wang, Yanhua Tao

Guidance and Simulation Lab, Rocket University of Engineering Precision, Xi'an, Shaanxi, China.

How to cite this paper: Shuo Yuan, Yang Guo, Shaobo Wang, Yanhua Tao. (2023) Considering the Cooperative Guidance Law of Multiple Vehicles in Detection Configuration. *Engineering Advances*, 3(5), 407-417.
DOI: 10.26855/ea.2023.10.004

Received: September 28, 2023
Accepted: October 25, 2023
Published: November 21, 2023

***Corresponding author:** Yang Guo, Guidance and Simulation Lab, Rocket University of Engineering Precision, Xi'an, Shaanxi, China.

Abstract

For the missing relative distance guidance problem, a cooperative guidance law for multiple vehicles considering the detection configuration is proposed. Firstly, to address the issue of missing relative distance, the relative distance can be determined by implementing cooperative detection using multiple interceptors. Secondly, considering that the configuration of interceptors can impact detection errors, the guidance law incorporates a cooperative ranging error model that is dependent on the line-of-sight separation angle between two interceptors. The guidance law also utilizes optimal control theory to design an optimal guidance law that can adjust the line-of-sight separation angle between the two interceptors. This adjustment allows for the separation of the trajectories of the two vehicles, thereby increasing their line-of-sight separation angles and reducing the cooperative detection errors of the two interceptors. After conducting a Monte Carlo simulation, the proposed guidance estimation method is compared to the traditional guidance estimation method. The results indicate that the proposed method outperforms the traditional method in terms of detection and interception performance.

Keywords

Multi-vehicle, cooperative interception, detection configuration, line-of-sight separation angle

1. Introduction

With the development and progress of military technology, the maneuvering form of the target is becoming more and more complex and variable, and its maneuvering and escaping capability has increased significantly, making it more and more difficult for individual interceptors to obtain more accurate target information in the game confrontation between the enemy and our aircraft, and the possibility of successfully capturing the target is getting lower and lower [1]. To obtain more accurate target information and achieve better interception performance, it is necessary to measure and estimate information other than the line-of-sight angle [2]. Such as target acceleration, approach speed, remaining time, and relative distance to the target, almost all of which depend on the relative distance information between the interceptor and the target, except for the line-of-sight angle and its rate of change [3]. Multi-vehicle cooperative target capture has strategic and quantitative advantages compared to single vehicle [4]. By cooperating with each other [5], the gaming countermeasures and detection and guidance accuracy can be greatly improved, thus successfully achieving cooperative interception of maneuvering targets [6].

In the process of intercepting a maneuvering target using multiple vehicles in concert, the relative geometric configuration of the vehicles during guidance affects the detection error of the target. When multiple vehicles are used to further estimate the distance information by cooperative angle measurement, the relative distance cannot be estimated if the multiple vehicles are co-linear with the target, and the estimation error is larger when they are approximately co-linear. Liu et al. gave a specific error model associated with the line-of-sight separation angle. The specific error model related to the line-of-sight separation angle is given by Liu et al. [7], which shows that the detection error of the two interceptors' cooperative ranging increases as the line-of-sight separation angle decreases, so it is necessary to modulate the flight

trajectories of the two interceptors in the cooperative guidance process so that they can be separated from each other to reduce the cooperative detection error. Based on the literature [8], Fonod et al. [9] introduced the detection error model proposed by Liu to extend the cooperative detection guidance problem to the case where the target launches two defenders in a cooperative counter-intercept seeking missile and investigated that the line-of-sight separation angle between the two defenders is between 30 and 65 degrees for them to have a better intercept performance. In addition, Fonod [10] designed a "blinding" guidance law based on optimal control theory and detection error model for the case of two interceptors cooperatively intercepting a maneuvering target, which makes the line-of-sight separation angle between the two interceptors smaller, and the guidance law can increase the detection error of the two interceptors cooperatively ranging to increase the intercept off-target. This law can increase the probability of survival by increasing the detection error between the two interceptors and increasing the amount of intercept off-target, combined with the bang-bang maneuver escape of the target. In the paper [11], based on the paper [9], an anti-interception guidance law is designed based on the optimal control for the deep cooperation between the target and the two defenders, which gives the optimal control input for the cooperation between the target and the two defenders considering three aspects: interception off-target amount, terminal bar interception angle and energy consumption.

From the existing domestic literature, most of the studies on cooperative guidance have considered the detection and guidance aspects separately, without analyzing the influence of the relative geometric configuration on the detection capability during the cooperative process of the vehicle. Therefore, in this paper, the influence of the relative configuration of the guidance on the detection accuracy is considered to investigate the design of the guidance law and the application of the detection estimation method.

In summary, based on the above literature, this paper proposes a cooperative guidance law that considers the detection configuration error model based on optimal control theory for the case of two interceptors cooperating to intercept a maneuvering target, which can modulate the line-of-sight separation angle of the two interceptors to reduce the detection error of the target.

2. Problem Description

Assume a scenario where two of our interceptors intercept an enemy target capable of performing a bang-bang optimal evasion maneuver. In this scenario, there are two important factors to consider: one is that the interceptors need to adopt an efficient estimation approach to detect random changes in the target and to accurately estimate the target state. The other is that the relative detection configurations of the two interceptors can affect the detection accuracy of the target state information.

Dynamics and kinematics are modeled in the inertial coordinate system at $X_I - O_I - Y_I$. Pi and E denote interceptors and maneuvering targets, respectively. a v, λ, r and γ represent the normal acceleration, velocity, line-of-sight angle, relative distance, and heading angle, respectively. The engagement motion model of the two interceptors and the maneuvering target is shown in Figure 1.

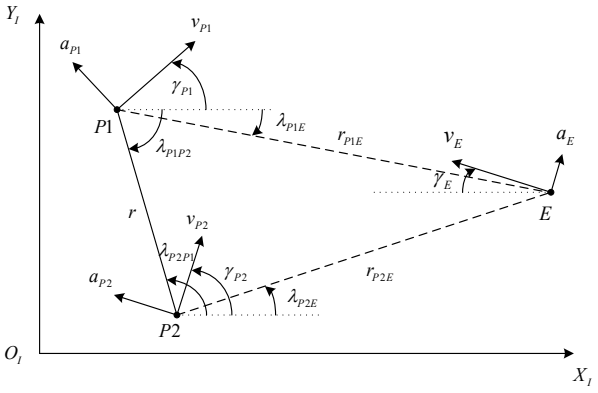

Figure 1. Plane engagement geometry.

2.1 Dynamics and kinematics models

Neglecting the effect of gravity, the engagement process between the interceptor and the maneuvering target can be expressed in the form of polar coordinates associated with the maneuvering target (r, λ), i.e.

$$\dot{r}_{PiE} = v_{PiE} = -v_E \cos\left(\gamma_E - \lambda_{PiE}\right) - v_{Pi} \cos\left(\gamma_{P_0} + \lambda_{PiE}\right); \quad i = \{1,2\} \tag{1}$$

$$\dot{\lambda}_{PiE}=\frac{v_E\sin\left(\gamma_E-\lambda_{PiE}\right)-v_{Pi}\sin\left(\gamma_{P_{i_0}}+\lambda_{PiE}\right)}{r_{PiE}};\quad i=\{1,2\} \tag{2}$$

Where: $\dot{r}_{PiE}$ is the relative velocity between the two vehicles; $\dot{\lambda}_{PiE}$ is the angular rate of the line-of-sight between the two vehicles.

Because the direction of acceleration is always perpendicular to the velocity direction throughout the guidance process, the velocities of the interceptor and the maneuvering target are always constant. Therefore, the relationship between the normal acceleration of the vehicle and the heading angle can be expressed as

$$\dot{\gamma}_i=\frac{a_i}{v_i};\quad i=\{E,P_1P_2\} \tag{3}$$

Note 1. The above process can be linearized when the flight processes of the two vehicles can be approximated as nominal collision triangles. Two collision triangles consisting of two pursuers each with a maneuvering target exist during the engagement depicted in Figure 1.

After linearizing the above process, we can choose the state vector

$$\boldsymbol{x}_i=\begin{bmatrix}x_1 & x_2 & x_3 & x_4\end{bmatrix}^T=\begin{bmatrix}y_i & \dfrac{dy_i}{dt} & a_E & a_{Pi}\end{bmatrix};\quad i=\{1,2\} \tag{4}$$

Where: $\overset{\Delta}{y_i}=y_E-y_{Pi}$ is the lateral distance between the interceptor P_i and the maneuvering target E, and $\dfrac{dy_i}{dt}$ is the lateral relative velocity.

Assuming that the interceptor and the maneuvering target can be approximated as a first-order dynamics model, the equation of state for the relative motion between the vehicles can be written as

$$\begin{cases}\dot{x}_1=x_2\\ \dot{x}_2=x_3-x_4\\ \dot{x}_3=\dfrac{a_E^c-x_3}{\tau_E};\quad i=\{1,2\}\\ \dot{x}_4=\dfrac{a_{Pi}^c-x_4}{\tau_{Pi}}\end{cases} \tag{5}$$

where τ_{Pi} and τ_E are the overload response time constants for interceptors and maneuvering targets, respectively.

Set of equations (5) of matrix form is

$$\dot{\boldsymbol{x}}_i=\boldsymbol{A}_i\boldsymbol{x}_i(t)+\boldsymbol{B}_iu_{Pi}(t)+\boldsymbol{C}a_E^c(t)+w(t);\quad i=\{1,2\} \tag{6}$$

Eq:

$\boldsymbol{A}_i=\begin{bmatrix}0&1&0&0\\0&0&1&-1\\0&0&\dfrac{-1}{\tau_E}&0\\0&0&0&\dfrac{-1}{\tau_{Pi}}\end{bmatrix}$, $\boldsymbol{B}=\begin{bmatrix}0\\0\\0\\\dfrac{1}{\tau_{Pi}}\end{bmatrix}$, $\boldsymbol{C}=\begin{bmatrix}0\\0\\\dfrac{1}{\tau_E}\\0\end{bmatrix}$, u_{Pi} are the control inputs of the pursuer and the constraints $\left|u_{Pi}\right|\le u_{Pi}^{\max}$ are satisfied. a_E^c is the commanded acceleration of the maneuvering target, and w is the noise of the guidance process.

The initial distance between the interceptor and the maneuvering target can be expressed as r_{P1E_0} and r_{P2E_0}. Under the assumption of nominal collision triangle, the deviation between the heading angle γ_i and the line-of-sight angle λ_{PiE} is small. Therefore, the interception time of the interceptor to the maneuvering target is constant and can be expressed as

$$t_{fPiE}=\frac{-r_{PiE_0}}{\dot{r}_{PiE_0}}=\frac{r_{PiE_0}}{v_E\cos\left(\gamma_{E_0}-\lambda_{PiE_0}\right)+v_{Pi}\cos\left(\gamma_{Pi_0}+\lambda_{PiE_0}\right)};\quad i=\{1,2\} \tag{7}$$

Note 2. In this paper, we consider the special case of two interceptors intercepting a maneuvering target at the same time, then their interception times are equal, *i.e.*, $t_{fP1E}=t_{fP2E}$. Therefore, the initial distances between them are also equal, i.e., $r_{P1E_0}=r_{P2E_0}$.

2.2 Measurement model

Each interceptor uses its own sensor to measure the line-of-sight angle λ_{PiE}. In addition, each sensor is interfered with by Gaussian white noise v_{Pi} and they are independent of each other. We assume that the line-of-sight measurement noise of each interceptor obeys the distribution

$$v_{Pi}^{\lambda}\sim N\left(0,\sigma_{Pi,\lambda}^2\right);\quad i\{1,2\} \tag{8}$$

As can be seen in Figure 1, during the engagement, the two interceptors are able to form a measurement baseline relative to the maneuvering target. Assuming that the interceptor is able to measure its relative state accurately and they are able to share their respective measurements with each other, the relative position information between them $\left(r,\lambda_{PiPj}\right)$, $i,j=1,2,i\neq j$ can be obtained.

Therefore, the relative distance between the two interceptors and the maneuvering target can be calculated from the known relative distance information of the two interceptors at r and the line-of-sight angle information at λ_{P1P2}

$$\tilde{r}_{PiE}=r\frac{\sin\left(\lambda_{P1P2}-\lambda_{PjE}\right)}{\sin\left(\lambda_{PiE}-\lambda_{PjE}\right)} \tag{9}$$

Eq:

$$r=\sqrt{\left(x_{P1}-x_{P2}\right)^2+\left(y_{P1}-y_{P2}\right)^2} \tag{10}$$

$$\lambda_{P1P2}=\arctan 2\left(y_{P2}-y_{P1},x_{P2}-x_{P1}\right) \tag{11}$$

Under linearization assumptions that satisfy the nominal collision triangle, the lateral displacement perpendicular to the initial line-of-sight angle y_i can be expressed as

$$y_i\approx\left(\lambda_{PiE}-\lambda_{PiE_0}\right)r_{PiE} \tag{12}$$

$$r_{PiE}\approx v_{PiE}t_{go} \tag{13}$$

Where: t_{go} is the remaining interception time.

$$t_{go}\overset{\Delta}{=}\begin{cases}t_{fPiE}-t, & t\le t_{fPiE}\\ 0, & t>t_{fPiE}\end{cases} \tag{14}$$

Combined formula (9), the measurement equation of the interceptor can be obtained

$$z_i=\boldsymbol{H}\boldsymbol{x}_i+v_{P_i}^{y}=y_i+v_{Pi}^{y} \tag{15}$$

Eq: $\boldsymbol{H}=\begin{bmatrix}1 & 0 & 0 & 0\end{bmatrix}$

$$v_{Pi}^{y}\sim N\left(0,\sigma_{Pi,y}^2\right) \tag{16}$$

$$\sigma_{Pi,y}=r\lambda_{PiE}\frac{\sqrt{\sin^2\left(\lambda_{P1P2}-\lambda_{PiE}\right)\sigma_{Pj,\lambda}^2+\sin^2\left(\lambda_{P1P2}-\lambda_{PjE}\right)\cos^2\left(\lambda_{PiE}-\lambda_{PjE}\right)\sigma_{Pi,\lambda}^2}}{\sin\left(\lambda_{PiE}-\lambda_{PjE}\right)} \tag{17}$$

Note 3. From equation (17) it is known that when the line-of-sight separation angle between the two interceptors

$\left|\lambda_{PiE}-\lambda_{PjE}\right|$ decreases, the measurement variance of the lateral displacement y_i will increase, leading to a decrease in the accuracy of the state estimation. Therefore, it is necessary to control the line-of-sight separation angle of the two interceptors relative to the target when designing the guidance law.

2.3 Performance indicators

Successful interception of a maneuvering target by an interceptor requires a very small amount of terminal off-target or a direct hit. However, interceptors are not able to hit maneuvering targets with high accuracy due to various factors. In particular, the method of estimating the state of the maneuvering target severely limits the interceptor's guidance accuracy. Because it is difficult to obtain hit models influenced by multiple factors in realistic operational environments, we utilize a simplified hit function to assess the likelihood of target destruction:

$$P_d\left(M,R_k\right)=\begin{cases}1 & M\le R_k\\ 0 & M>R_k\end{cases} \tag{18}$$

The off-target quantity, an indicator of intercept success, is affected by the random maneuvers of the target and the measurement noise of the detection process, and therefore, the off-target quantity is a randomly varying quantity. We usually use the Cumulative Distribution Function (CDF) as an empirical estimate to evaluate the effect of off-target quantity on guidance accuracy and use it to compare the guidance performance between different guidance laws. Thus, we can determine whether the interception is successful by using a predetermined probability of kill for a given LR condition. The hit probability can be defined as

$$\mathrm{SSKP}(R_k)=\mathrm{E}\{P_d(M,R_k)\} \tag{19}$$

Where: E is the mathematical expectation about the off-target quantity random variable. The CDF can be calculated by SSKP, which is given by

$$\begin{aligned}\mathrm{SSKR}\left(R_k\right)&=\int_{-\infty}^{\infty}P_d\left(M,R_k\right)f_M\left(m\right)\\&=\int_0^{R_k}f_M\left(m\right)dm=pr\left(M\le R_k\right)\overset{\Delta}{=}F_M\left(R_k\right)\end{aligned} \tag{20}$$

Where: f_M and F_M are the Probability Density Function PDF (Probability Density Function) and CDF, respectively. The interception probability is generally taken as 0.95, and the performance index can be obtained as follows

$$J=\underset{R_k}{\arg}\left\{\mathrm{SSKR}\left(R_k\right)=0.95\right\} \tag{21}$$

3. Co-Guided Law Design

In this section, we give a more specific description of the engagement problem from Section 1. The main factor considered in the design of the guidance law is that the guidance configuration of the vehicle can affect the detection accuracy of the target, i.e., the line-of-sight separation angle between the two interceptors can affect the measurement variance of the relative distance. If the guidance law cannot control the line-of-sight angle, the line-of-sight separation angle between the two interceptors may become smaller, which in turn leads to an increase in detection error. Therefore, our interceptor needs to control the line-of-sight separation angle at the end of the guidance so that it can meet the requirements of detection and guidance accuracy. If the interceptor with the larger initial line-of-sight angle maximizes its line-of-sight angle and the other minimizes its line-of-sight angle, the line-of-sight separation angle between the two interceptors will become larger and the estimated accuracy will be enhanced.

We use optimal control theory to achieve the above-mentioned cooperative guidance by taking off-target volume and energy consumption into account.

3.1 Objective function

Under the assumption of nominal collision triangles, the lateral displacement of the interceptor can be approximated as

$$y_i\approx\left(\lambda_{PiE}-\lambda_{PiE_0}\right)r_{PiE} \tag{22}$$

$$\lambda_{PiE}\approx v_{PiE}t_{go} \tag{23}$$

Combined formula (22) and (23), the line-of-sight angle λ_{PiE} can be approximated as

$$\lambda_{PiE} \approx \lambda_{PiE_0} + \frac{y_i}{v_{PiE} t_{go}} \tag{24}$$

Introducing the term $\frac{y_i}{t_{go}}$, the **performance** index of the optimal control can be established as

$$J^y = \frac{1}{2} a_i y_i^2 \left(t_f\right) + \frac{1}{2} b_i \int_{t_k}^{t_f} u_{Pi}^2 d\tau + \frac{1}{2} c_i \int_{t_k}^{t_f} \frac{y_i \left(t_f\right)}{t_{go} + \Delta t} d\tau \tag{25}$$

Note 4. We use instead of $\frac{y_i \left(t_f\right)}{t_{go} + \Delta t} \frac{y_i \left(t_f\right)}{t_{go}}$ to avoid the singularity of calculating and deriving formulas later. When is used, $\Delta t \to 0$ $\frac{y_i \left(t_f\right)}{t_{go} + \Delta t} \to \frac{y_i \left(t_f\right)}{t_{go}}$. We make $a \to \infty$, we can get the off-target amount tending to 0 for the governing law. Note that the line-of-sight angle will be minimized if the weights $c_i > 0$ and maximized if $c_i < 0$ Define abbreviations and acronyms the first time they are used in the text, even after they have been defined in the abstract. Abbreviations such as IEEE, SI, MKS, CGS, sc, dc, and rms do not have to be defined. Do not use abbreviations in the title or heads unless they are unavoidable.

3.2 Descending order

In order to reduce the order of solving the optimization problem and to obtain an analytical solution for the control inputs, we introduce the terminal projection method for order reduction. This requires us to introduce new state variables defined as

$$Z_i \left(t\right) = \boldsymbol{D\Phi}_i \left(t_f, t\right) \boldsymbol{x}_i \left(t\right) \tag{26}$$

$$\dot{\boldsymbol{\Phi}}_i \left(t_f, t\right) = -\dot{\boldsymbol{\Phi}}_i \left(t_f, t\right) \boldsymbol{A}_i \tag{27}$$

Combined formula (27) and the derivatives of the new state variables with respect to time, we are able to obtain

$$\begin{aligned} \dot{Z}_i \left(t\right) &= \boldsymbol{D}\dot{\boldsymbol{\Phi}}_i \left(t_f, t\right) \boldsymbol{x}_i \left(t\right) + \boldsymbol{D\Phi}_i \left(t_f, t\right) \dot{\boldsymbol{x}}_i \left(t\right) \\ &= \boldsymbol{D\Phi}_i \left(t_f, t\right) \boldsymbol{B}_i u_{Pi} \left(t\right) \end{aligned} \tag{28}$$

Formula (28) shows that $\dot{Z}_i \left(t\right)$ is state-independent and only relevant to the designed controller, in addition, we label $\boldsymbol{D\Phi}_i \left(t_f, t\right) \boldsymbol{B}_i$ as $\hat{B}_i$.

Using the terminal projection method to reduce the order, the objective function (25) by a new representation of the state variables

$$J^Z = \frac{1}{2} a_i Z_i^2 \left(t_f\right) + \frac{1}{2} b_i \int_{t_k}^{t_f} u_{Pi}^2 d\tau + \frac{1}{2} c_i \int_{t_k}^{t_f} \frac{Z \left(t_f\right)}{t_{go} + \Delta t} d\tau \tag{29}$$

3.3 Optimal controller s

The Hamiltonian function for the performance metric is

$$H = \frac{1}{2} b_i u_{Pi}^2 + \frac{1}{2} c_i \frac{Z_i \left(t\right)}{t_{go}} + \lambda_Z \dot{Z}_i \left(t\right) \tag{30}$$

The derivatives of the new state variables with respect to time are state-independent, thus greatly simplifying the accompanying equations.

$$\dot{\lambda}_Z = -\frac{\partial H}{\partial Z_i} = -\frac{c_i}{2 t_{go}} \tag{31}$$

$$\lambda_Z\left(t_f\right)=a_iZ_i\left(t_f\right) \tag{32}$$

Combining the equation (31) from t_f to t and integrate Eq. (32) into the equation gives

$$\lambda_Z\left(t\right)=a_iZ_i\left(t_f\right)+\frac{1}{2}c_i\ln\frac{t_{go}}{\Delta t} \tag{33}$$

From the control equation we get

$$\begin{aligned}&\frac{\partial H}{\partial u_{Pi}}=0\Rightarrow\\&u_{Pi}=-\frac{\hat{B}_i}{b_i}\left[a_iZ_i\left(t_f\right)+\frac{c_i}{2}\ln\frac{t_{go}}{\Delta t}\right]\end{aligned} \tag{34}$$

The equation (34) into equation (28) we get

$$\dot{Z}_i\left(t\right)=-\frac{\hat{B}_i^2}{b_i}a_iZ_i\left(t_f\right)-\frac{c_i\hat{B}_i^2}{2b_i}\ln\frac{t_{go}}{\Delta t} \tag{35}$$

Putting the equation (35) Integrating from t to t_f yields

$$Z_i\left(t_f\right)-Z_i\left(t\right)=-\frac{a_i}{b_i}Z_i\left(t_f\right)\hat{B}_{i1}-\frac{c_i}{2b_i}\hat{B}_{i2} \tag{36}$$

Where: $\hat{B}_{il}=\int_t^{t_f}\hat{B}_i^2d\tau$, $\hat{B}_{i2}=\int_t^{t_f}\hat{B}_i^2\ln\frac{t_{go}}{\Delta t}d\tau$.

Therefore, we can solve $Z_i\left(t_f\right)$ for

$$Z_i\left(t_f\right)=\frac{Z_i\left(t\right)-\frac{c_i}{2b_i}\hat{B}_{i2}}{1+\frac{a_i}{b_i}\hat{B}_{il}} \tag{37}$$

Substitute $Z_i\left(t_f\right)$ into equation (34) in the equation, the optimal controller can be solved

$$u_{Pi}=-\hat{B}_i\left[\frac{Z_i\left(t\right)-\frac{c_i}{2b_i}\hat{B}_{i2}}{\frac{b_i}{a_i}+\hat{B}_{il}}+\frac{c_i}{2}\ln\frac{t_{go}}{\Delta t}\right] \tag{38}$$

When $a\to\infty$, a perfect interception guidance law with 0 interception off-target is obtained, i.e.

$$u_{Pi}=-\hat{B}_i\left[\frac{Z_i\left(t\right)-\frac{c_i}{2b_i}\hat{B}_{i2}}{\hat{B}_{il}}+\frac{c_i}{2}\ln\frac{t_{go}}{\Delta t}\right] \tag{39}$$

4. Simulation Analysis

In this section, we perform numerical simulations to verify the proposed cooperative guidance law and IMM filtering. First, we set the simulation parameters and initially analyze the engagement scenarios of the three vehicles. Then, we explore the effects of the cooperative guidance law and the IMM filter on the maneuvering target detection and guidance performance, and we evaluate them by introducing Monte Carlo (MC). There are two main factors affecting the interceptor guidance and detection performance: one is the detection configuration of the two interceptors during guidance; the other is the detection capability of the IMM filter on the target maneuver switching time. Finally, we compare the proposed cooperative guidance law using the IMM filter with this guidance law using Kalman filter with shaping filter (KF/SF) and the extended proportional guidance guidance law (APNG) using the IMM filter.

4.1 Simulation Parameters and Engagement Scenarios

For the guidance law designed in Section 2, the simulation parameters are set as follows: interceptor 1 and interceptor 2 are launched simultaneously, and the initial distance to the maneuvering target are both $y_{PiE_0} = 12000$ m. The initial lateral displacements are $y_{P1E_0} = -50m$ and $y_{P2E_0} = 50m$ The velocities of interceptor and target are $v_{Pi} = 2000m/s$ and $v_E = 1000$ m/s, respectively. Ignoring the effect of gravity, the overload limits of interceptor and target are $u_{Pi}^{\max} = 68g$ and $a_E^{\max} = 12g$, respectively, and the overload response time constants are $\tau_{Pi} = 0.2s$ and $\tau_E = 0.2s$, respectively. The simulation time interval is set to $\Delta = 0.001$ s, and the standard deviation of the line-of-sight angle measurement noise is $\sigma_E^{\max} = 1$ mrad.

Figure 2 shows the engagement diagram of interceptor 1 and interceptor 2 cooperatively intercepting a maneuvering target. It can be seen from the figure that the proposed cooperative guidance law is able to modulate the trajectories of the two interceptors so that they are separated from each other to increase their line-of-sight separation angles, thus avoiding detection errors caused by the guidance configuration. Figure 3 shows the acceleration variation of the two interceptors, from which it can be seen that the acceleration of both interceptors does not exceed the overload limit. Combined with Figure 2 and Figure 3, Interceptor 2 does not require higher maneuvering capability because it does not require larger maneuvering, while Interceptor 1 has to cooperate with Interceptor 2 to increase the line-of-sight separation angle between them, so compared with the initial state advantage of Interceptor 2, Interceptor 1 needs to pay a greater maneuvering cost to achieve the guidance purpose.

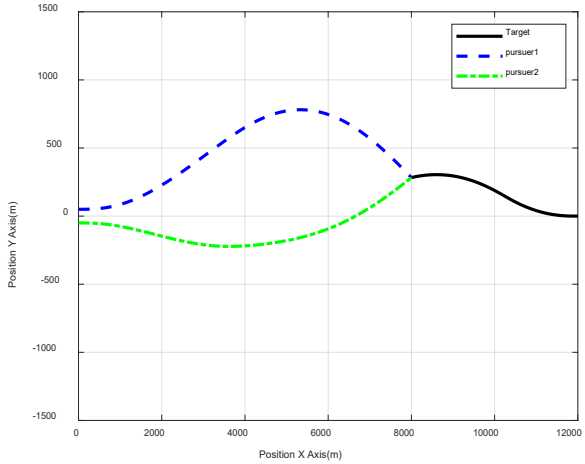

Figure 2. Multi-aircraft coordinated interception engagement.

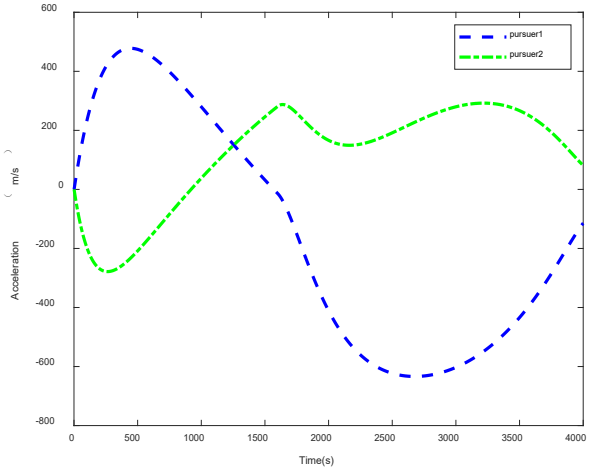

Figure 3. Acceleration variation of the interceptor.

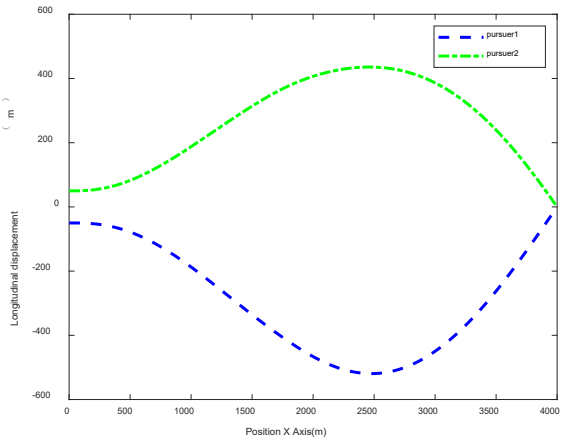

Figure 4. Interceptor longitudinal displacement.

Figure 5 shows the angular variation of the line-of-sight separation angle between the two interceptors for different guidance laws and estimation methods. Comparing the two plots, it can be seen that using the APN combined with the IMM method results in a small line-of-sight separation angle throughout the guidance process, which leads to a large detection error noise because the APN cannot control the line-of-sight separation angle between the two vehicles. As can be seen in Fig. 4, the proposed guidance law can control the line-of-sight separation angle between the two vehicles, and it can make the line-of-sight separation angle increase gradually.

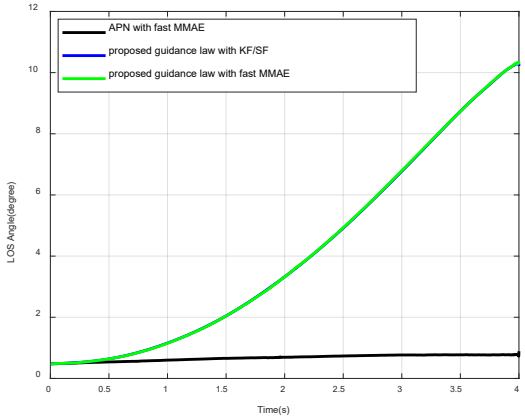

Figure 5. LOS separation angle between interceptors in APN combined with IMM, the proposed guidance law combined with KF/SF and IMM.

4.2 Off-target volume assessment

In this subsection, we analyze the closed-loop intercept performance of the APN combined with the IMM, the proposed guidance law combined with the KF/SF, and the IMM by introducing 100 MC simulations. Figures 6 and 7 show the off-target volume CDF for both interceptors, and Table 1 summarizes the range of combatant kills required to ensure a 95% kill probability for both interceptors. For Interceptor 1, for example, the proposed guidance law combined with IMM requires only 0.81m kill range compared to the APN combined with IMM which requires 9.47m kill range and the proposed guidance law combined with KF/SF which requires 22.86m kill range. As shown in Figs. 6 and 7, the intercept performance of the proposed guidance law combined with IMM is better than the other two guidance and estimation methods. Furthermore, comparing Figures 6 and 7, the method of estimating acceleration using the IMM results in approximate intercept performance for both intercepts, and they are relatively close in the range of combatant kill required to ensure a 95% probability of kill. In contrast, the method using the KF/SF estimated acceleration results in a large difference in the interception performance of the two interceptors, with a large difference in their required combatant kill ranges, partly due to the inaccurate estimation of acceleration and partly due to the higher cost of maneuvering required for interceptor 1.

Table 1. Required Warhead Lethality Ranges of Pure Predictive Guidance Law, Apn^{MMSE}, and Proposed Guidance Law to Ensure a 95% Kill Probability

Guidance law and estimation method	Pursuer1, m	Pursuer2, m
APN with fast MMAE	9.74	7.14
Proposed guidance law with KF/SF	22.86	1.35
Proposed guidance law with fast MMAE	0.81	0.39

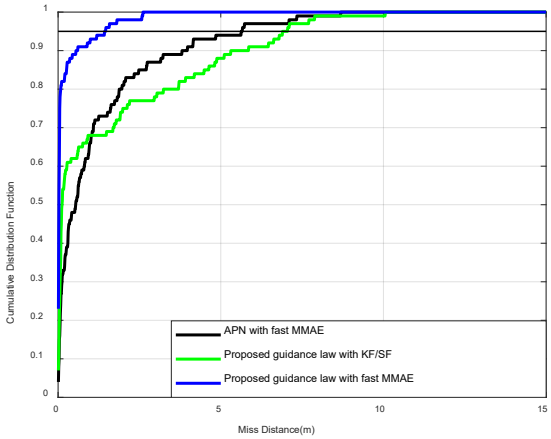

Figure 6. Miss distance cumulative distribution function of interceptor1 in the APN combined with IMM, proposed guidance law combined with KF/SF, and proposed guidance law combined with IMM.

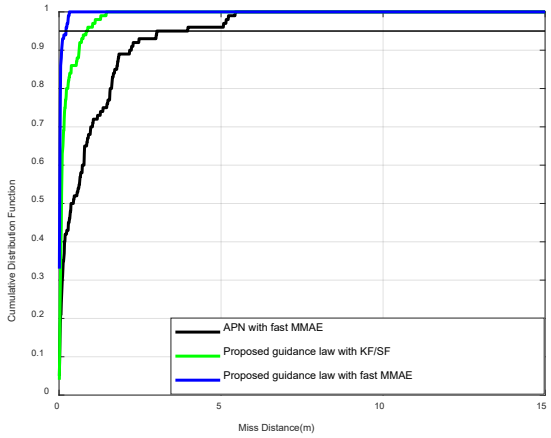

Figure 7. Miss distance cumulative distribution function of interceptor2 in the APN combined with IMM, proposed guidance law combined with KF/SF, and proposed guidance law combined with IMM.

5. Conclusion

For the missing relative distance guidance problem, a cooperative guidance law for multiple vehicles considering the detection configuration is proposed. By introducing multi-interceptor cooperative detection to obtain the relative distance, and secondly, considering that the detection configuration of interceptors affects the detection error, the guidance law introduces a cooperative ranging error model related to the line-of-sight separation angle of two interceptors, and adopts the optimal control theory to design an optimal guidance law that can modulate the line-of-sight separation angle of two interceptors, which can separate the trajectories of two vehicles to increase their line-of-sight separation angle to reduce the two interceptors. The two interceptors can be detected together. After Monte Carlo simulation, the proposed guidance estimation method is compared with the traditional guidance estimation method, and the results show that the proposed guidance estimation method has obvious advantages in detection and interception performance compared with the traditional method.

References

[1] Hexner G, Weiss H, Dror S. Temporal Multiple Model Estimator for a Maneuvering Target [C]//AIAA Guidance, Navigation, and Control Conference. Honolulu, Hawaii, 2008: 2008-7456.

[2] Guo Zhiqiang, Zhou Shaolei. Research on Cooperative Differential Game Guidance Law for Multi-Missile [J]. Journal of Sichuan Ordnance. 2019, 40(5): 21-25.

[3] Chen Z, Yu J, X Dong, et al. Three-dimensional cooper-ative guidance strategy and guidance law for intercepting highly maneuvering target [J]. Chinese Journal of Aeronautics, 2021, 34(5):485-495.

[4] Yu J L, Dong X W, Li Q D, et al. Distributed Cooperative Encirclement Hunting Guidance Method for intercepting the Maneuvering Target [J]. Acta Aeronautica et Astronautica Sinica, 2021, 42:325817.

[5] Shima T, Oshman Y, Shinar J. Efficient Multiple Model Adaptive Estimation in Ballistic Missile Interception Scenarios [J]. Journal of Guidance, Control, and Dynamics. 2002, 25(4): 667-675.

[6] Zhang S, Guo Y, Lu Z X, et al. Cooperative Detection Based on the Adaptive Interacting Multiple Model-Information Filtering Algorithm [J]. Aerospace Science and Technology, 2019, 93.

[7] Liu Y F, Qi N M, Shan J J. Cooperative Interception with Double-Line-of-Sight-Measuring [C]// Proceedings of AIAA Guidance, Navigation, and Control Conference. Boston, MA, US: AIAA, 2013: 2013-5112.

[8] Shaferman V, Shima T. Cooperative Optimal Guidance Laws for Imposing a Relative Intercept Angle [J]. Journal of Guidance, Control, and Dynamics, 2015, 38(8): 1395-1408.

[9] Fonod R, Shima T. Estimation Enhancement by Cooperatively Imposing Relative Intercept Angles [J]. Journal of Guidance, Control, and Dynamics, 2017, 40(7): 1711-1725.

[10] Fonod R, Shima T. Blinding Guidance Against Missiles Sharing Bearings-Only Measurements [J]. IEEE Transactions on Aerospace and Electronic Systems, 2018, 54(1): 205-216.

[11] Julier S, Uhlmann J, Durrant-Whyte H F. A New Method for the Nonlinear Transformation of Means and Covariances in Filters and Estimators [J]. IEEE Transactions on Automatic Control, 2000, 45(3): 477-482.